Defining the Design Space for Double–Double Laminates by Considering Homogenization Criterion

Kai Zhao* and David Kennedy†
Cardiff University, Cardiff, Wales CF24 3AA, United Kingdom
Antonio Miravete‡
Massachusetts Institute of Technology, Cambridge, Massachusetts 02139
Stephen W. Tsai§
Stanford University, Stanford, California 94305-4035
Carol A. Featherston¶
Cardiff University, Cardiff, Wales CF24 3AA, United Kingdom
and
Xiaoyang Liu**
Qingdao University of Technology, 266033 Qingdao, People's Republic of China

https://doi.org/10.2514/1.J062639

The double–double (DD) laminate families that contain two continuous angles, which were proposed by Tsai ("Double–Double: New Family of Composite Laminates," *AIAA Journal*, Vol. 59, No. 11, 2021, pp. 4293–4305), opened up a whole new era for composite layups, which are easy to manufacture and design. In the present study, the design space referred to as feasible regions is derived explicitly based on novel formulations for the lamination parameters of DD laminates. This enables the boundaries of the design space to be obtained analytically, providing mathematical support for DD families. The obtained result shows that their design space is larger than that of conventional quadaxial laminates in terms of industrial practices. A homogenization criterion is implemented into the design space, based on which a tailored DD laminate is proposed, expanding design possibilities and enabling homogenization to be achieved using only 16 plies/4 repeats. The work proposed offers significant benefits through practical solutions to making design, manufacturing, and testing simpler and more competitive.

I. Introduction

CONVENTIONAL composite laminates comprise a collection of 0, ±45, and 90 deg plies (known as quadaxial or QUAD) [1]. These layups have been used since the 1960s, when boron and high-strength carbon fiber composites were developed [2]. By changing lamina directions and stacking sequences, a large number of permutations of QUAD laminates are possible, allowing them to meet the majority of application requirements. To ensure manufacturability and enhance damage tolerance, a number of layup design rules are generally applied, e.g., midplane symmetry, the 10% rule, blending, etc. [3,4]. This results in a complex optimization design process. To achieve the application requirements and minimize the weight of the laminate, the design of QUAD laminates (especially when ply drop-offs are considered) is now not as simple as its four-angle concept. Instead, it has become more complicated and, as a result, more time consuming [5–10].

The double–double (DD) laminates proposed by Tsai [1] are a new family of composite laminates that consist of a repeat of a four-ply sublaminate. Four types of DD laminates that are commonly referred to as staggered 1, staggered 2, staggered 3, and paired have been proposed. The corresponding stacking sequences of their sublaminate are $[+\phi/-\psi/-\phi/+\psi]$, $[+\phi/+\psi/-\phi/-\psi]$, $[+\phi/-\psi/+\psi/-\phi]$, and $[\pm\phi/\pm\psi]$, respectively, in which ϕ and ψ are two continuous ply angle variables ranging from 0 to 90 deg. The usage of DD laminates avoids several issues in the design of composite laminates. Homogenization in the thickness direction is one of the key advantages allowing DD laminates to be much more lightweight as compared to QUAD layups [1]. This is because when a laminate is homogenized, which is achieved by stacking the sublaminate, its in-plane/out-of-plane coupling can be intrinsically ignored [11]. As a result, the optimization of DD laminates can be performed without imposing the midplane symmetry rule, removing a large number of plies. Traditional QUAD laminates, on the other hand, are heterogeneous, requiring at least 120 plies or 15 mm to be homogenized [1]. For the optimization design of composite laminates with varying thicknesses, a QUAD laminate requires plies in symmetrical positions to be dropped simultaneously to avoid warping [12]. Without the need to consider midplane symmetry, the tapering of DD laminates can be achieved more easily by dropping plies from one side, placed on the exterior surfaces of laminates [13]. In addition to homogenization, with only two continuous design variables (unbalanced laminates have one more angle variable as a rigid-body rotation), DD laminates are extremely easy to optimize; whereas QUAD layups have millions of permutations in terms of angles and stacking sequences when the number of plies reaches 10 or more [12]. Designing the tapering of such a high number of plies would not even be possible.

From the perspective of practical manufacturing, as mentioned earlier, DD laminates possess a nonstop layup without midplane symmetry. Such a feature is beneficial to improving the efficiency of the fabrication process and the quality of the laminates [1]. Besides, a QUAD laminate is a collection of discrete laminates; whereas DD laminates are field based, making manipulation easy because of the continuous function. Because plies can be dropped in singles from one side, all the plies in the interior are parallel and stacked continuously, reducing the probability of voids, wrinkles, and warpage in the manufacturing process [13].

Tsai [1] concluded that DD laminates could achieve a similar performance to most QUAD designs by taking advantage of

Received 12 November 2022; revision received 12 February 2023; accepted for publication 13 February 2023; published online Open Access 8 March 2023.

*Research Associate, School of Engineering.
†Professor, School of Engineering. Senior Member AIAA.
‡Research Affiliate, Department of Aeronautics and Astronautics.
§Professor Research Emeritus, Department of Aeronautics and Astronautics.
¶Professor, School of Engineering.
**Associate Professor, School of Civil Engineering, Shandong; liuxiaoyang@qut.edu.cn (Corresponding Author).

their larger design spaces. Lamination parameters [14–17] that are independent of the number of plies in the laminates can be used to present these design spaces, which are more commonly referred to as feasible regions. However, the explicit and specific boundaries of the feasible region of DD laminates have never been found. This is a significant limitation because the feasible regions are treated as design constraints in the lamination parameter optimization, and obtaining their boundaries is essential to the optimum design process. York [18] discovered that the lower bound of the design space of lamination parameters ξ_1^A, ξ_2^A and ξ_1^D, ξ_2^D for general two-angle laminates can be represented by parabolas. However, the upper bound of design spaces for other lamination parameters, especially the in-plane/out-of-plane coupling parameters (i.e. $\xi_{1,2,3,4}^B$), which are key parameters to determine the homogenization, have not been discussed. Therefore, the extension of the homogenization of DD laminates has not been defined mathematically, resulting in sacrificing the design space for the near-homogenized laminates.

In this paper, taking advantage of the repetition in DD laminates, formulations for obtaining the lamination parameters of DD laminates are derived: based on which, the lamination parameters can be expressed in simple forms. The proposed formulations are not limited to the most commonly used DD laminate sequence, i.e., staggered 1. They are also applicable to DD laminates with rigid-body rotation: unbalanced DD laminates that have four different angles (i.e., adding an extra angle parameter to each sublaminate). With the aid of these formulations, a method based on Lagrange multipliers is proposed to derive the feasible regions of any combination of two lamination parameters. Benefiting from the simple expressions for the lamination parameters, all feasible regions are obtained analytically. Based on the obtained feasible regions, clear insight into the homogenization of a DD laminate is visualized and parametrized. Furthermore, the effect of the number of plies on the homogenization is investigated based on the homogenization criterion defined in Ref. [1]. The work proposed offers practical solutions, making the design, manufacturing, and testing simpler and more competitive.

Section II introduces the conventional way of calculating lamination parameters, whereas the new expressions for the lamination parameters of DD laminates are given in Sec. III. Section IV describes the method for analytically obtaining the feasible regions of DD laminates as well as the obtained results. Brief conclusions are given in Sec. V.

II. Lamination Parameters

Lamination parameters were first introduced by Tsai and Pagano in 1968 [19], enabling the stiffness matrix to be represented by a linear function and significantly reducing the number of design variables. For the design of either flat or curved composite laminates, lamination parameters can be used as design variables instead of the large number of ply angles to meet the mechanical requirements of engineering scenarios with regard to buckling, postbuckling, vibration, etc. [20]. By using lamination parameters as design variables, the number of design variables can be reduced to a maximum of 12; the stiffness matrix can then be expressed as a linear function of these lamination parameters instead of the conventional set of equations with a large number of ply orientations [21].

Based on classical laminate theory, the stress–strain relationship for a composite laminate can be expressed as

$$\begin{bmatrix} \boldsymbol{n} \\ \boldsymbol{m} \end{bmatrix} = \begin{bmatrix} \boldsymbol{A} & \boldsymbol{B} \\ \boldsymbol{B} & \boldsymbol{D} \end{bmatrix} \begin{bmatrix} \boldsymbol{\varepsilon}^0 \\ \boldsymbol{\kappa} \end{bmatrix} \tag{1}$$

where $\boldsymbol{n}$ and $\boldsymbol{m}$ are vectors of the in-plane forces and moments per unit width; $\boldsymbol{A}$, $\boldsymbol{B}$ and $\boldsymbol{D}$ are the in-plane, coupling, and out-of-plane stiffness matrices; $\boldsymbol{\varepsilon}^0$ is a vector of in-plane strains; and $\boldsymbol{\kappa}$ is a vector of midplane curvatures.

The stiffness matrices $\boldsymbol{A}$, $\boldsymbol{B}$, and $\boldsymbol{D}$ can be expressed in terms of 12 lamination parameters $\xi_j^k (j = 1, 2, 3, 4; k = A, B, D)$ and material stiffness invariants $\boldsymbol{u}$ as shown in the following:

$$\begin{bmatrix} A_{11} \\ A_{22} \\ A_{12} \\ A_{66} \\ A_{16} \\ A_{26} \end{bmatrix} = h \begin{bmatrix} 1 & \xi_1^A & \xi_2^A & 0 & 0 \\ 1 & -\xi_1^A & \xi_2^A & 0 & 0 \\ 0 & 0 & -\xi_2^A & 1 & 0 \\ 0 & 0 & -\xi_2^A & 0 & 1 \\ 0 & \xi_3^A/2 & \xi_4^A & 0 & 0 \\ 0 & \xi_3^A/2 & -\xi_4^A & 0 & 0 \end{bmatrix} \begin{bmatrix} U_1 \\ U_2 \\ U_3 \\ U_4 \\ U_5 \end{bmatrix} \tag{2}$$

$$\begin{bmatrix} B_{11} \\ B_{22} \\ B_{12} \\ B_{66} \\ B_{16} \\ B_{26} \end{bmatrix} = \frac{h^2}{2} \begin{bmatrix} 0 & \xi_1^B & \xi_2^B & 0 & 0 \\ 0 & -\xi_1^B & \xi_2^B & 0 & 0 \\ 0 & 0 & -\xi_2^B & 0 & 0 \\ 0 & 0 & -\xi_2^B & 0 & 0 \\ 0 & \xi_3^B/2 & \xi_4^B & 0 & 0 \\ 0 & \xi_3^B/2 & -\xi_4^B & 0 & 0 \end{bmatrix} \begin{bmatrix} U_1 \\ U_2 \\ U_3 \\ U_4 \\ U_5 \end{bmatrix} \tag{3}$$

$$\begin{bmatrix} D_{11} \\ D_{22} \\ D_{12} \\ D_{66} \\ D_{16} \\ D_{26} \end{bmatrix} = \frac{h^3}{12} \begin{bmatrix} 1 & \xi_1^D & \xi_2^D & 0 & 0 \\ 1 & -\xi_1^D & \xi_2^D & 0 & 0 \\ 0 & 0 & -\xi_2^D & 1 & 0 \\ 0 & 0 & -\xi_2^D & 0 & 1 \\ 0 & \xi_3^D/2 & \xi_4^D & 0 & 0 \\ 0 & \xi_3^D/2 & -\xi_4^D & 0 & 0 \end{bmatrix} \begin{bmatrix} U_1 \\ U_2 \\ U_3 \\ U_4 \\ U_5 \end{bmatrix} \tag{4}$$

where the material stiffness invariants $\boldsymbol{u}$ and the stiffness properties $\boldsymbol{Q}$ are

$$\begin{bmatrix} U_1 \\ U_2 \\ U_3 \\ U_4 \\ U_5 \end{bmatrix} = \frac{1}{8} \begin{bmatrix} 3 & 3 & 2 & 4 \\ 4 & -4 & 0 & 0 \\ 1 & 1 & -2 & -4 \\ 1 & 1 & 6 & -4 \\ 1 & 1 & -2 & 4 \end{bmatrix} \begin{bmatrix} Q_{11} \\ Q_{22} \\ Q_{12} \\ Q_{66} \end{bmatrix} \tag{5}$$

$$\begin{cases} Q_{11} = E_{11}/(1 - \nu_x \nu_y) \\ Q_{22} = E_{22}/(1 - \nu_x \nu_y) \\ Q_{12} = \upsilon_x Q_{22} \\ Q_{66} = G_{12} \end{cases} \tag{6}$$

where E_{11} is the longitudinal Young's modulus; E_{22} is the transverse modulus; G_{12} is the shear modulus; υ_x and υ_y; are the major and minor Poisson's ratios, respectively; and h is the thickness of the laminate.

The lamination parameters are obtained by the following integrals:

$$\begin{bmatrix} \xi_1^k \\ \xi_2^k \\ \xi_3^k \\ \xi_4^k \end{bmatrix} = \int_{-h/2}^{h/2} Z^k \begin{bmatrix} \cos 2\theta \\ \cos 4\theta \\ \sin 2\theta \\ \sin 4\theta \end{bmatrix} \mathrm{d}z, \quad k = A, B, D, \begin{cases} Z^A = 1/h \\ Z^B = 2z/h^2 \\ Z^D = 12z^2/h^3 \end{cases} \tag{7}$$

where θ represents the ply angle at depth z below the midsurface. For a general angle laminate, such an equation cannot be simplified further because the angle of each ply differs at different depths.

III. Lamination Parameters of General DD Laminates

Because the sublaminate of the DD laminates has only four angles [namely, two angles with opposite signs or four different angles [1]

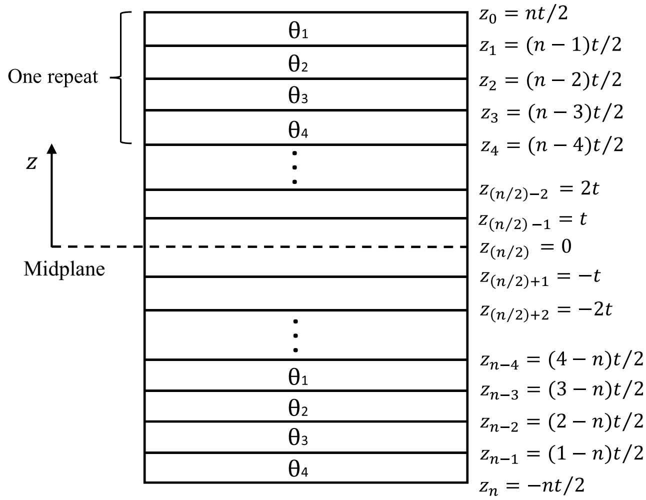

Fig. 1 General DD laminates and locations of each node through the thickness.

(i.e., unbalanced DD laminates)], Eq. (7) can be derived with respect to the four angles: θ_1, θ_2, θ_3, and θ_4.

Assuming a laminate has n plies with thickness t identified by $n+1$ nodes and comprising $n/4$ repetitions of sublaminate $[\theta_1, \theta_2, \theta_3, \theta_4]$, for which the locations are shown in Fig. 1, it should be noted that the total number of layers n is always an even number; and the midplane always lies on the boundary of two plies.

Then, for $k = 1, 2, \ldots, n/4$, the kth repetition has its top surface at $z = t[-1/2 + (4k-4)/n]$ and its bottom surface at $z = t[-1/2 + (4k)/n]$.

Thus, the kth θ_1 ply runs from $z = t[-1/2 + (4k-4)/n]$ to $z = t[-1/2 + (4k-3)/n]$; the kth θ_2 ply runs from $z = t[-1/2 + (4k-3)/n]$ to $z = t[-1/2 + (4k-2)/n]$; the kth θ_3 ply runs from $z = t[-1/2 + (4k-2)/n]$ to $z = t[-1/2 + (4k-1)/n]$; and the kth θ_4 ply runs from $z = t[-1/2 + (4k-1)/n]$ to $z = t[-1/2 + (4k)/n]$.

Defining trigonometric functions $f_1(\theta) = \cos(2\theta)$, $f_2(\theta) = \cos(4\theta)$, $f_3(\theta) = \sin(2\theta)$, and $f_4(\theta) = \sin(4\theta)$, the lamination parameters $\xi^{A,B,D}_{1,2,3,4}$ can be calculated as follows:

For $\xi^A_{1,2,3,4}$, Eq. (7) can be expressed as

$$\begin{bmatrix} \xi^A_1 \\ \xi^A_2 \\ \xi^A_3 \\ \xi^A_4 \end{bmatrix} = \int_{-nt/2}^{nt/2} \frac{1}{nt} \begin{bmatrix} f_1(\theta) \\ f_2(\theta) \\ f_3(\theta) \\ f_4(\theta) \end{bmatrix} \mathrm{d}z \tag{8}$$

Integrating each ply through the thickness,

$$\begin{aligned} \xi^A_j = \frac{1}{t} \sum_{k=1}^{n/4} \Bigg\{ & \int_{t[-1/2+(4k-4)/n]}^{t[-1/2+(4k-3)/n]} f_j(\theta_1)\,\mathrm{d}z + \int_{t[-1/2+(4k-3)/n]}^{t[-1/2+(4k-2)/n]} f_j(\theta_2)\,\mathrm{d}z \\ & + \int_{t[-1/2+(4k-2)/n]}^{t[-1/2+(4k-1)/n]} f_j(\theta_3)\,\mathrm{d}z + \int_{t[-1/2+(4k-1)/n]}^{t[-1/2+(4k)/n]} f_j(\theta_4)\,\mathrm{d}z \Bigg\} \end{aligned} \tag{9}$$

Simplifying Eq. (9), we have

$$\xi^A_j = \left\{ \frac{1}{4} f_j(\theta_1) + \frac{1}{4} f_j(\theta_2) + \frac{1}{4} f_j(\theta_3) + \frac{1}{4} f_j(\theta_4) \right\} \tag{10}$$

It can be seen that equal contributions are made by all four of the angles. So, for the DD laminates without rigid-body rotation, the contributions based on cosine functions will be equal and opposite so that ξ^A_3 and ξ^A_4 are zero.

For $\xi^B_{1,2,3,4}$, similar to Eq. (8), substituting the number of plies n and thicknesses t into Eq. (7), we have

$$\begin{bmatrix} \xi^B_1 \\ \xi^B_2 \\ \xi^B_3 \\ \xi^B_4 \end{bmatrix} = \int_{-nt/2}^{nt/2} \frac{2z}{(nt)^2} \begin{bmatrix} f_1(\theta) \\ f_2(\theta) \\ f_3(\theta) \\ f_4(\theta) \end{bmatrix} \mathrm{d}z \tag{11}$$

Integrating each ply through the thickness,

$$\begin{aligned} \xi^B_j = \frac{2}{t^2} \sum_{k=1}^{n/4} \Bigg\{ & \int_{t[-1/2+(4k-4)/n]}^{t[-1/2+(4k-3)/n]} z f_j(\theta_1)\mathrm{d}z + \int_{t[-1/2+(4k-3)/n]}^{t[-1/2+(4k-2)/n]} z f_j(\theta_2)\mathrm{d}z \\ & + \int_{t[-1/2+(4k-2)/n]}^{t[-1/2+(4k-1)/n]} z f_j(\theta_3)\,\mathrm{d}z + \int_{t[-1/2+(4k-1)/n]}^{t[-1/2+(4k)/n]} z f_j(\theta_4)\,\mathrm{d}z \Bigg\} \end{aligned} \tag{12}$$

and simplifying,

$$\xi^B_j = \left\{ -\frac{3}{n} f_j(\theta_1) - \frac{1}{n} f_j(\theta_2) + \frac{1}{n} f_j(\theta_3) + \frac{3}{n} f_j(\theta_4) \right\} \tag{13}$$

It can be seen that the contributions are inversely proportional to the number of plies n so that increasing the number of plies can restrict the magnitude of the ξ^B_j lamination parameters to any required limit, i.e., approximating a symmetric laminate.

For $\xi^D_{1,2,3,4}$, Eq. (7) can be rewritten as

$$\begin{bmatrix} \xi^D_1 \\ \xi^D_2 \\ \xi^D_3 \\ \xi^D_4 \end{bmatrix} = \int_{-nt/2}^{nt/2} \frac{12z^2}{(nt)^3} \begin{bmatrix} f_1(\theta) \\ f_2(\theta) \\ f_3(\theta) \\ f_4(\theta) \end{bmatrix} \mathrm{d}z \tag{14}$$

Integrating each ply through the thickness,

$$\begin{aligned} \xi^D_j = \frac{12}{t^3} \sum_{k=1}^{n/4} \Bigg\{ & \int_{t[-1/2+(4k-4)/n]}^{t[-1/2+(4k-3)/n]} z^2 f_j(\theta_1)\,\mathrm{d}z \\ & + \int_{t[-1/2+(4k-3)/n]}^{t[-1/2+(4k-2)/n]} z^2 f_j(\theta_2)\,\mathrm{d}z + \int_{t[-1/2+(4k-2)/n]}^{t[-1/2+(4k-1)/n]} z^2 f_j(\theta_3)\,\mathrm{d}z \\ & + \int_{t[-1/2+(4k-1)/n]}^{t[-1/2+(4k)/n]} z^2 f_j(\theta_4)\,\mathrm{d}z \Bigg\} \end{aligned} \tag{15}$$

and simplifying,

$$\begin{aligned} \xi^D_j = \Bigg\{ & \left(\frac{1}{4} + \frac{3}{n^2}\right) f_j(\theta_1) + \left(\frac{1}{4} - \frac{3}{n^2}\right) f_j(\theta_2) + \left(\frac{1}{4} - \frac{3}{n^2}\right) f_j(\theta_3) \\ & + \left(\frac{1}{4} + \frac{3}{n^2}\right) f_j(\theta_4) \Bigg\} \end{aligned} \tag{16}$$

As can be seen from Eqs. (10), (13), and (16), each set of lamination parameters ($\xi^A_{1,2,3,4}$, $\xi^B_{1,2,3,4}$, and $\xi^D_{1,2,3,4}$) can be obtained through a single equation, in contrast to the integral equations that need to be solved for QUAD layups, making the feasible regions easier to obtain.

It can be observed from the preceding equations that the values of $\xi^A_{1,2,3,4}$ are related only to the ply angles; hence, increasing the number of plies in DD laminates has no effect on their in-plane lamination parameters. Besides, $\xi^B_{1,2,3,4}$ are inversely proportional to the number of plies and $\xi^D_{1,2,3,4}$ are inversely proportional to the square of the number of plies. As a result, as the number of plies increases, $\xi^B_{1,2,3,4}$ decreases with a first-order relation, whereas $\xi^D_{1,2,3,4}$ decreases with a second-order one. These relations are impossible to explicitly describe for QUAD layups due to the complexity of their stacking sequences. On the other hand, such explicit expressions can be very advantageous when deriving the boundaries of the design space in terms of lamination parameters, as will be shown in the following sections.

IV. Feasible Regions of DD Laminates

A. Feasible Regions of General DD Using Lagrange Multiplier

The feasible regions of the lamination parameters are treated as constraints when employing lamination parameters as nondimensional design variables [22–35]. The earliest work on feasible regions of lamination parameters was by Miki [36,37], who defined the feasible region for the in-plane or out-of-plane stiffness of an orthotropic laminate. After that, the feasible regions of the four in-plane or four out-of-plane lamination parameters of symmetric laminates were determined in Fukunaga and Sekine's works [38,39]. In the work of Diaconu et al. [40], the feasible regions in the general design space of all 12 of the lamination parameters were first presented and found to be finite convex spaces. Later, Setoodeh et al. [41] developed a method to approximate the boundaries of the general feasible region for lamination parameters using the method of convex hulls. Bloomfield et al. [14] developed closed-form solutions to define the feasible regions of any predefined finite orientation set. These studies focused on the three four-dimensional spaces defining in-plane, coupling, and flexural stiffnesses. Linking between them, however, has not been considered due to the highly nonlinear nature of this problem. Such nonlinear links constrain the algebraic relationships between the three design spaces, further increasing the complexity of the convex polyhedron describing the design space [42]. Researchers have been pushing the boundary of feasible regions of lamination parameters to exploit any possible stiffness tailoring of a laminate through either new methodologies or representations of feasible regions. However, research on the boundaries of the design space highly depends on replacing or adding constraints regardless of the methods used, leading to more complex design space.

Compared to QUAD layups, the design complexity of DD laminates is significantly reduced due to the simple stacking concept. Furthermore, the design spaces corresponding to DD laminates are found to be larger than those corresponding to QUAD layups in industrial practice, which will be proved later in this paper.

This section describes a methodology to obtain the feasible regions of combinations of any two lamination parameters for DD laminates (i.e., staggered 1: $[+\phi/-\psi/-\phi/\psi]$, staggered 2: $[+\phi/+\psi/-\phi/-\psi]$, staggered 3: $[+\phi/-\psi/+\psi/-\phi]$, and Paired: $[\pm\phi/\pm\psi]$) without rigid-body rotation, using Lagrange multipliers, in favor of simplifying composite design.

To obtain the feasible regions of any two lamination parameters for DD laminates, we plot one of the parameters along the horizontal x axis and find the minimum and maximum possible values of the other parameter y. A constrained optimization problem can therefore be summarized in the following form:

Minimize and maximize $y = f(\theta_{1,}\theta_2)$ subject to $x = g(\theta_{1,}\theta_2)$, where f and g denote the functions of θ_1, θ_2.

Solutions correspond to the stationary values of the augmented function

$$F(\theta_1, \theta_2, \lambda) = f(\theta_1, \theta_2) + \lambda(g(\theta_1, \theta_2) - x) \tag{17}$$

where λ is a Lagrange multiplier.

The conditions to be satisfied at each stationary point are

$$\frac{\partial F}{\partial \theta_1} = \frac{\partial f}{\partial \theta_1} + \lambda \frac{\partial g}{\partial \theta_1} = 0 \tag{18}$$

$$\frac{\partial F}{\partial \theta_2} = \frac{\partial f}{\partial \theta_2} + \lambda \frac{\partial g}{\partial \theta_2} = 0 \tag{19}$$

$$\frac{\partial F}{\partial \lambda} = g(\theta_{1,}\theta_2) - x = 0 \tag{20}$$

Solving Eqs. (18–20), the boundaries of the feasible region for any combination of nonzero lamination parameters for any DD laminate can be found. The key to solving the preceding equations depends largely on pairs of $\cos 2\theta$, $\sin 2\theta$, $\cos 4\theta$, and $\sin 4\theta$ in Eqs. (10), (13), and (16), from which it can be deduced that there are, by the combination rule, $C(4, 2) + 4 = 10$ solution types in total, as shown in Appendix A, where four are pairs of their own. Furthermore, the coefficients of Eqs. (10), (13), and (16) can potentially reduce the complexity of solving the preceding equations, depending on the type of DD laminates.

B. Feasible Regions of Staggered 1

In this section, one of the DD laminates presented by Tsai [1], which has sublaminates with the stacking sequence $[+\phi/-\psi/-\phi/+\psi]$, will be taken as an example to validate the method proposed. Based on Eqs. (10), (13), and (16), $\xi^A_{1,2,3,4}$ can be written as

$$\begin{aligned}
\xi^A_1 &= \frac{1}{2}\cos(2\phi) + \frac{1}{2}\cos(2\psi);\\
\xi^A_2 &= \frac{1}{2}\cos(4\phi) + \frac{1}{2}\cos(4\psi);\\
\xi^A_3 &= 0; \quad \xi^A_4 = 0
\end{aligned} \tag{21}$$

It can be seen from Eq. (21) that equal contributions are made by the four plies. Therefore, in a DD laminate comprising angles $(\pm\phi, \pm\varphi)$, the contributions based on sine functions will be equal and opposite so that $\xi^A_{3,4}$, which are related to the shear–extension coupling stiffness, are intrinsically zeros. It should be noted that DD laminates could include shear–extension coupling when the plies are rotated; however, research on the DD laminates with ply rotation is out of the scope of this study. As for $\xi^B_{1,2,3,4}$, they can be expressed as

$$\begin{aligned}
\xi^B_1 &= -\frac{1}{2n}\cos(2\phi) + \frac{1}{2n}\cos(2\psi);\\
\xi^B_2 &= -\frac{1}{2n}\cos(4\phi) + \frac{1}{2n}\cos(4\psi);\\
\xi^B_3 &= -\frac{1}{n}\sin(2\phi) + \frac{1}{n}\sin(2\psi);\\
\xi^B_4 &= -\frac{1}{n}\sin(4\phi) + \frac{1}{n}\sin(4\psi)
\end{aligned} \tag{22}$$

It can be observed that the magnitudes of these lamination parameters are inversely proportional to the number of plies n so that increasing the number of plies will decrease the magnitude of $\xi^B_{1,2,3,4}$ to any required limit, i.e., approximating a symmetric laminate. Hence, homogeneity can be approximated to any required accuracy by increasing the number of plies. Expressions for $\xi^D_{1,2,3,4}$ are given in Eq. (23):

$$\begin{aligned}
\xi^D_1 &= \frac{1}{2}\cos(2\phi) + \frac{1}{2}\cos(2\psi)\\
\xi^D_2 &= \frac{1}{2}\cos(4\phi) + \frac{1}{2}\cos(4\psi)\\
\xi^D_3 &= \frac{6}{n^2}\sin(2\phi) + \frac{6}{n^2}\sin(2\psi)\\
\xi^D_4 &= \frac{6}{n^2}\sin(4\phi) + \frac{6}{n^2}\sin(4\psi)
\end{aligned} \tag{23}$$

The feasible regions of all possible combinations of any two lamination parameters are analytically obtained based on the preceding equations using the method of the Lagrange multipliers. However, in this method, constraints on ϕ and ψ are impossible to add because they will cause transcendental functions that have to be solved numerically. Such an approach will require a lot of computational effort and might not reach enough accuracy, which is not the intention of this paper. Therefore, ϕ and ψ are supposed to vary between -90 and 90 deg herein, which covers three DD laminates (i.e., staggered 1, staggered 2, and a part of paired). Based on this range, the obtained feasible regions can be used as base solutions for each type of DD laminate; the results of staggered 1, which is the most promising DD laminate, are presented in the following paragraphs. According to the combination rule, there are 66 solutions in total, i.e., $C(12, 2) = 66$. From Eqs. (21) and (23), we see that $\xi_1^A = \xi_1^D$, $\xi_2^A = \xi_2^D$, and $\xi_{3,4}^A = 0$, reducing the total number of combinations to 28, i.e., C(8,2). Although 28 solutions can be derived, there are only five basic solution types/unique region shapes, as shown in Fig. 2, with the rest of the 28 solutions being obtained from these by either rotation or scaling.

Figure 2 illustrates feasible regions of the five unique pairs of lamination parameters (i.e., $\xi_1^A - \xi_2^A/\xi_1^D - \xi_2^D$, ξ_1^A–ξ_1^B, ξ_1^B–ξ_2^B, ξ_1^B–ξ_3^B, and ξ_3^B–ξ_4^B). Five different shapes of feasible regions are obtained from six different types of solutions. The equations for the boundaries that include straight lines, quadratics, ellipses, and quartics are also included in the figure, with the equations being in the same color as the corresponding boundaries. To validate the obtained feasible regions, the lamination parameters of all of the possible layups for eight-ply laminates with ply angle increments of 1 deg are plotted (the blue scatter points) and can be seen to lie within the feasible region boundaries.

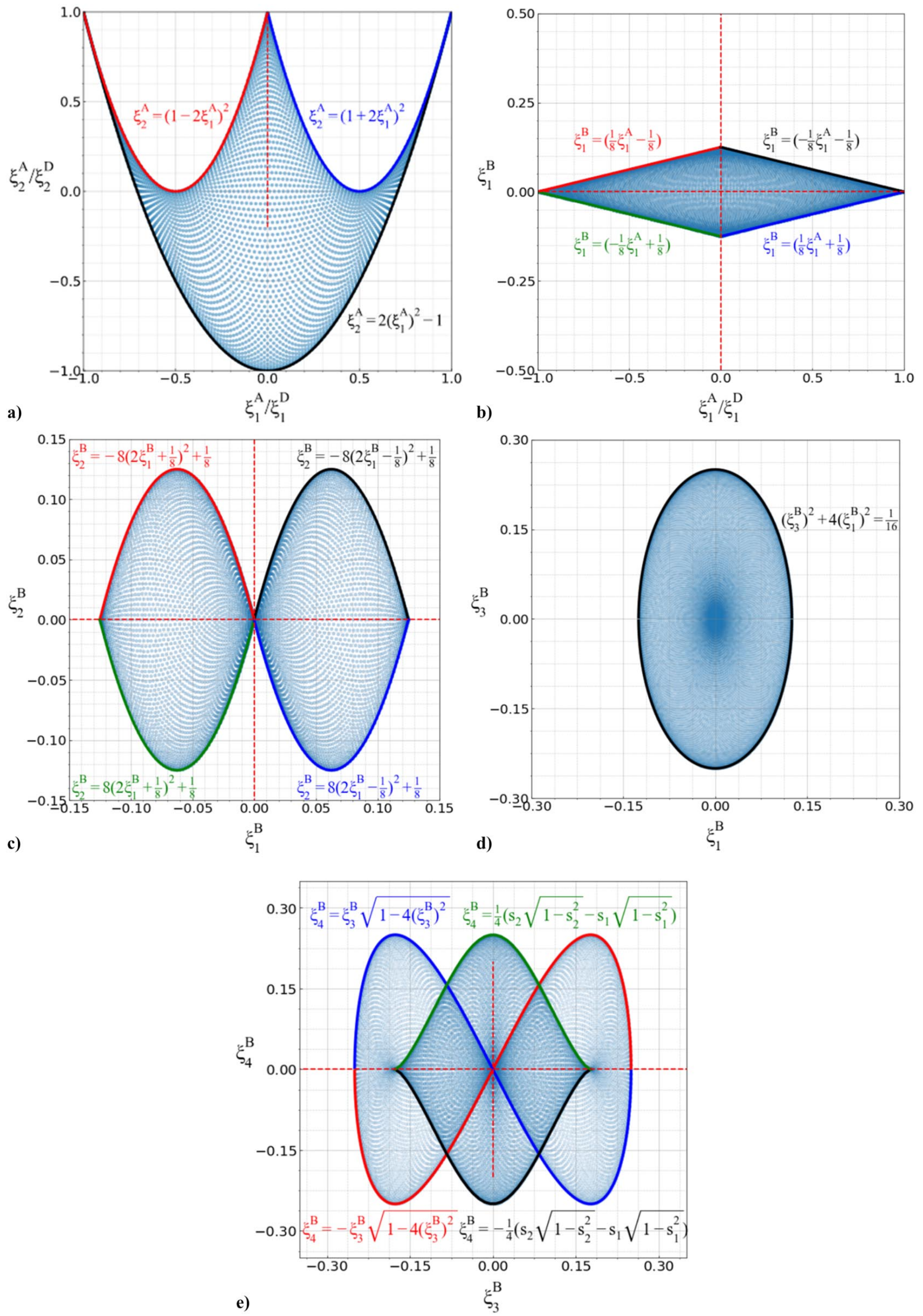

Fig. 2 Two-dimensional feasible regions of eight-ply laminate: six unique shapes.

The aforementioned solution covers larger design possibilities than each type of DD family. However, most of the types bring extra disadvantageous design space in coupling stiffness. It was found in Ref. [1] that the optimal sublaminate is the staggered 1. Such a configuration retains the same design space of in-plane and out-of-plane stiffnesses and has the minimum space for coupling stiffness. To obtain its feasible regions, extra constraints restricting angles lying within 0 to 90 deg must be added on the top of the base solutions. Those extra boundaries can be easily found by restricting one of the DD angles to be 0 or 90 deg. From Eqs. (21–23), it can be deducted that restricting ϕ and ψ to be positive only changes lamination parameters $\xi^B_{3,4}$ and $\xi^D_{3,4}$. Therefore, the feasible regions not related to these four lamination parameters are the same as the base solutions, which are shown in Appendix B. Such a method can be applied to any sequence of DD families.

Figure 3 illustrates unique shapes of feasible regions for staggered 1 marked in yellow scatters with eight plies in total, and their solutions are listed within plots. Because staggered 1 has different values of $\xi^B_{3,4}$ and $\xi^D_{3,4}$ as compared with the base solutions, 22 feasible regions related to them are changed. Among these feasible regions, six unique and basic shapes are identified, as shown in Figs. 3a–3f. It can be observed that restricting ϕ and ψ between

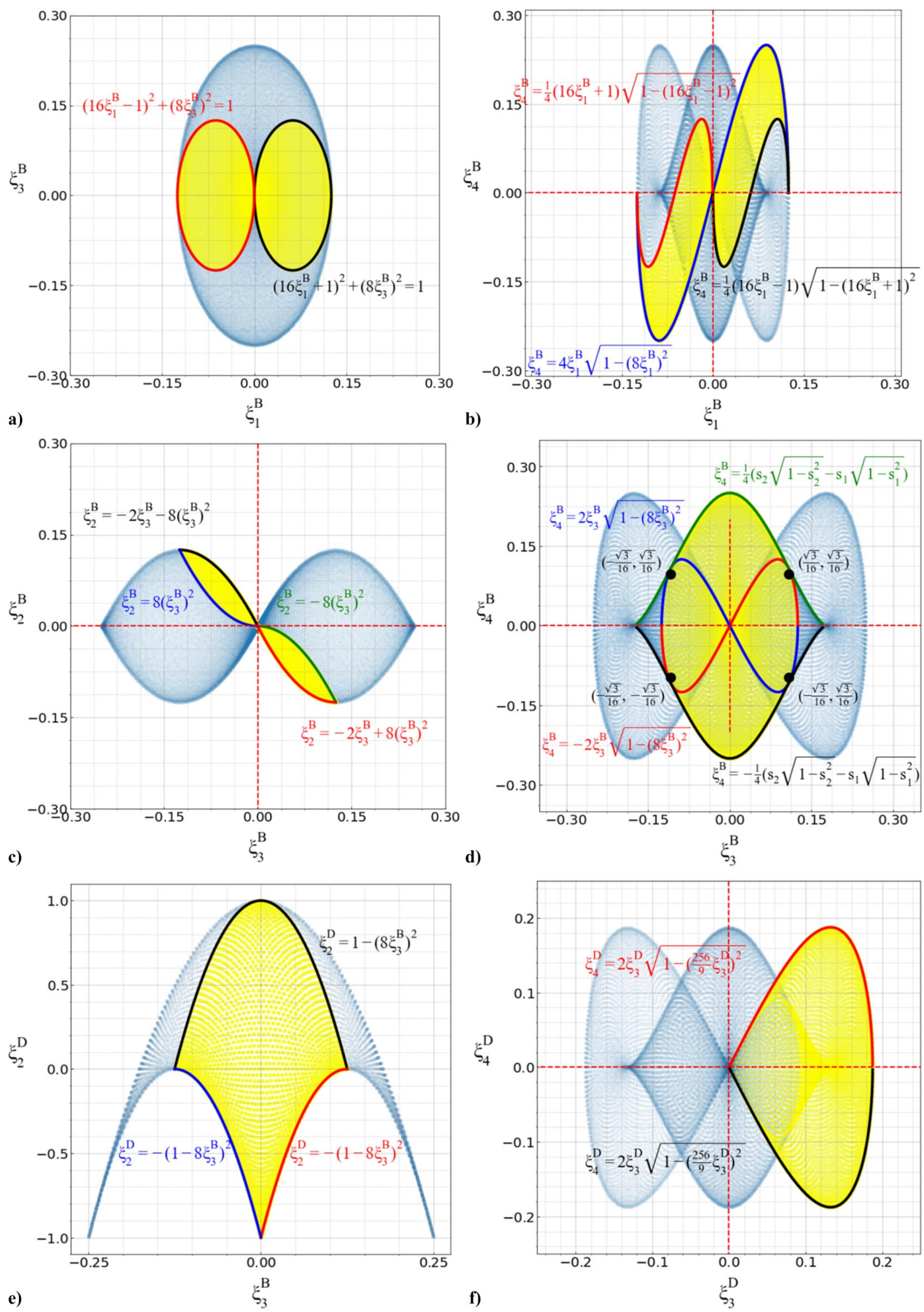

Fig. 3 Feasible regions for staggered 1 with eight plies.

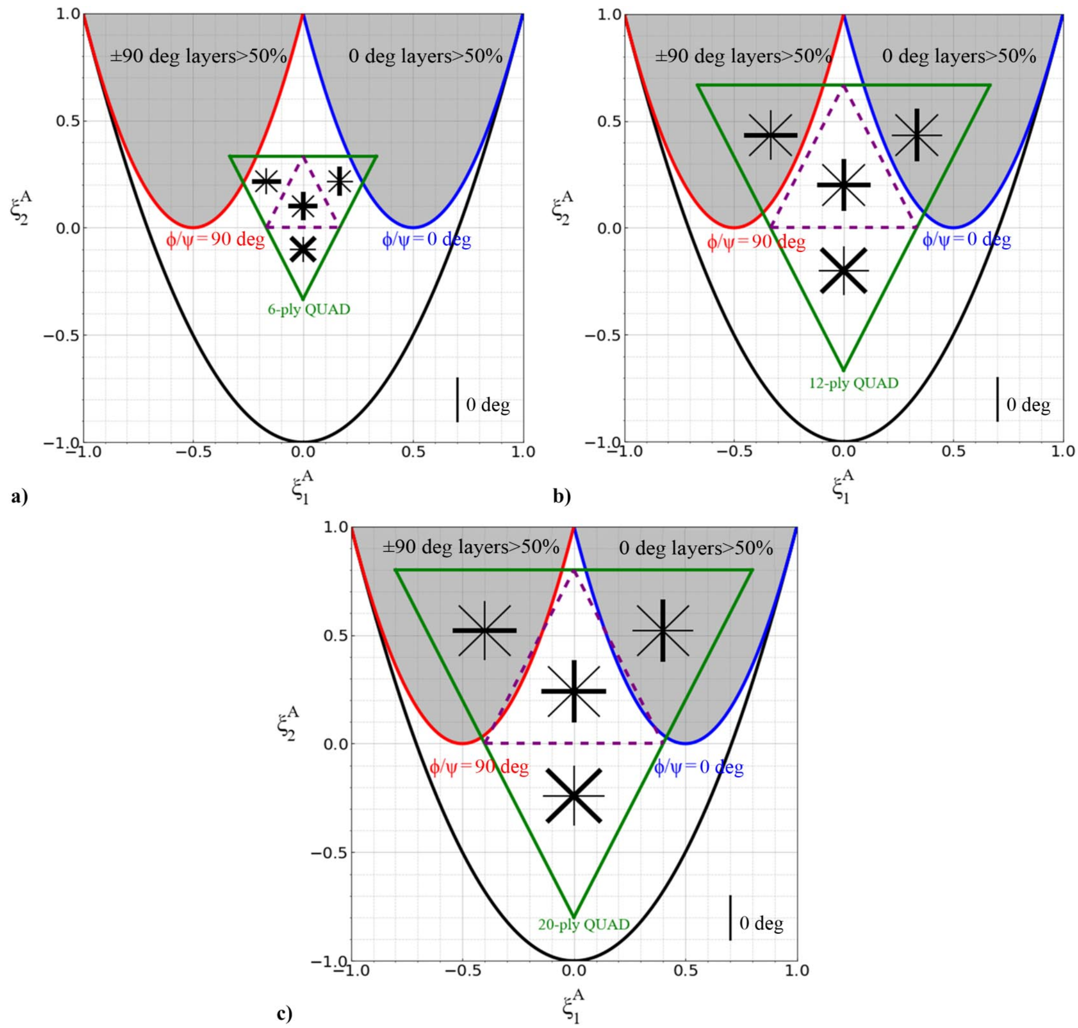

Fig. 4 Feasible region of ξ_1^A–ξ_2^A for DD laminates and QUAD laminates: a) 6 plies, b) 12 plies, and c) 20 plies.

0 and 90 deg significantly reduces the feasible regions of coupling lamination parameters $\xi^B_{1,2,3,4}$ as compared with the base solutions marked in blue scatters; hence, the coupling effect on staggered 1 is reduced.

Comparisons of the feasible region of ξ_1^A–ξ_2^A between QUAD laminates and DD laminates are shown in Fig. 4. The solid green lines in Figs. 4a–4c represent the feasible regions of 6-ply, 12-ply, and 20-ply QUAD laminates, respectively. It can be seen that the lower boundaries of the feasible region of DD laminates are lower than those of the three QUAD laminates, achieving more design possibilities. However, DD laminates cannot reach the lamination parameters located in the top left and top right of the feasible region of the QUAD laminates, especially when the number of plies is large. The red parabola represents the boundary above which the percentage of 90 deg plies should be more than 50% (hard laminates), whereas the blue parabola is the same for the 0 deg plies (hard laminates). Due to the nature of DD laminates, the maximum percentage of 90 or 0 deg is 50%. As shown in Fig. 4b, for QUAD laminates with a ply number of less than 12, which are mostly adopted in the industry, most of the feasible region can be covered by DD laminates and the rest can be approximated by the nearest point of DD laminates. For QUAD laminates with a large number of plies, the regions of soft laminates (±45 deg plies are more than 50%) and neutral laminates can still be fully covered. The hard laminates of the QUAD laminates, however, cannot be covered by DD laminates. To cover this area, some strategies can be applied to DD laminates, e.g., replacing the QUAD laminate by a DD laminate with the same A11*, A22*, or A66*, which are defined in Eq. (24). Besides, the failure envelopes of the hard QUAD laminates and approximated DD laminates are close. Hence, this reduction of the feasible region has only a small effect on DD laminates in terms of practical design.

For practical design, the coupling stiffness $\boldsymbol{B}$ is an important concern because it causes warping within a laminate. For QUAD laminates, the coupling stiffness is forced to be zero by stacking laminas symmetrically, resulting in high thickness laminates. Due to the nature of DD laminates, their coupling stiffness $\boldsymbol{B}$ cannot be eliminated. However, the coupling effect can be significantly reduced by increasing the number of plies. Such a phenomenon is known as homogenization [13]. Figure 5 shows the effect of the number of plies on the feasible regions of $\xi^B_{1,2,3,4}$. Because the boundaries of the feasible regions of DD laminates are inversely proportional to the number of plies (see Table 1), a DD laminate is able to achieve homogenization with only a few repeats. As can be seen from Fig. 5, the values of $\xi^B_{1,2,3,4}$ are halved when the number of plies is doubled. The maximum absolute values of $\xi^B_{3,4}$ for a DD laminate with eight plies are both 0.5, whereas those of a DD laminate with 32 plies are reduced to 0.125, which means the effects of B_{16} and B_{26} could be neglected. Compared to $\xi^B_{3,4}$, $\xi^B_{1,2}$ have even smaller absolute values. As can be seen from Fig. 5a, the maximum absolute values of $\xi^B_{1,2}$ for a DD laminate with 32 plies are less than 0.1.

On the other hand, homogenization is also seen for ξ_3^D and ξ_4^D because the contributions made by each angle are equal, with discrepancies that are inversely proportional to the square of the number of plies. Thus, the coupling parameters ξ_3^D and ξ_4^D are approaching zero when the number of plies increases (see Fig. 5g); whereas for QUAD laminates, these stiffnesses have to be tailored in order to avoid such coupling, which limits their design space.

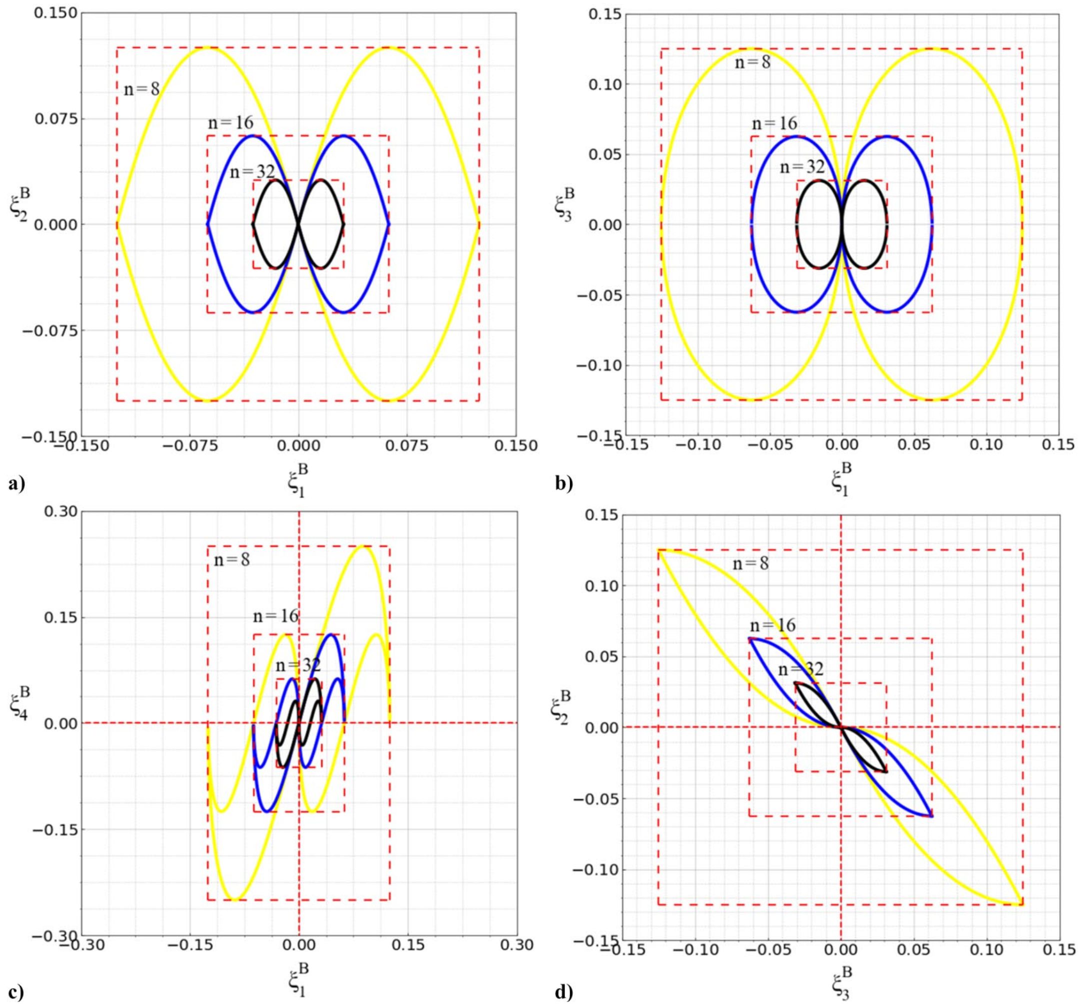

Fig. 5 Feasible regions of lamination parameters: a) ξ_1^B–ξ_2^B, b) ξ_1^B–ξ_3^B, c) ξ_1^B–ξ_4^B, d) ξ_3^B–ξ_2^B, e) ξ_2^B–ξ_4^B, f) ξ_3^B–ξ_4^B, and g) ξ_3^D–ξ_4^D.

C. Homogenization Criterion

According to Ref. [12], two criteria have to be met to reach homogenization, which require the largest components of $[\boldsymbol{B}^*]$ to be sufficiently small; and, $|[\boldsymbol{A}^*]-[\boldsymbol{D}^*]|$ is approaching 0[12], where $[\boldsymbol{A}^*,\boldsymbol{B}^*,\boldsymbol{D}^*]$ are the thickness normalized stiffnesses defined in Eq. (24) [43]:

$$\boldsymbol{A}^*,\boldsymbol{B}^*,\boldsymbol{D}^* = \left[\frac{1}{h}A_{ij}, \frac{2}{h^2}B_{ij}, \frac{12}{h^3}D_{ij}\right] \tag{24}$$

Specific homogenization criterion is defined in Ref. [1], i.e., a percentage I of the absolute value of the Tsai modulus [43] that can be defined in the following equations:

$$|\boldsymbol{B}_{ij}^*| < I * \text{Tsai modulus} \tag{25}$$

$$|[\boldsymbol{A}^*]-[\boldsymbol{D}^*]| < I * \text{Tsai modulus} \tag{26}$$

As for the DD laminates with a sublaminate of $[+\phi/-\psi/-\phi/+\psi]$, as $\xi_{1,2}^A = \xi_{1,2}^D$ and $\xi_{3,4}^A = 0$, with Eq. (25), it can be easily deduced that $A_{11}^*, A_{22}^*, A_{66}^* = D_{11}^*, D_{22}^*, D_{66}^*$ and $A_{16}^*, A_{26}^* = 0$. Hence, Eq. (27) can be simplified as

$$|[\boldsymbol{D}_{16}^*]| < I * \text{Tsai modulus} \tag{27}$$

$$|[\boldsymbol{D}_{26}^*]| < I * \text{Tsai modulus} \tag{28}$$

Normalizing Eq. (3) following Eq. (24), $\boldsymbol{B}^* = (2/h^2)\boldsymbol{B}$ so that

$$\begin{bmatrix} B_{11}^* \\ B_{22}^* \\ B_{12}^* \\ B_{66}^* \\ B_{16}^* \\ B_{26}^* \end{bmatrix} = \begin{bmatrix} 0 & \xi_1^B & \xi_2^B & 0 & 0 \\ 0 & -\xi_1^B & \xi_2^B & 0 & 0 \\ 0 & 0 & -\xi_2^B & 0 & 0 \\ 0 & 0 & -\xi_2^B & 0 & 0 \\ 0 & \xi_3^B/2 & \xi_4^B & 0 & 0 \\ 0 & \xi_3^B/2 & -\xi_4^B & 0 & 0 \end{bmatrix} \begin{bmatrix} U_1 \\ U_2 \\ U_3 \\ U_4 \\ U_5 \end{bmatrix} \tag{29}$$

Because the values of the components in stiffness matrix $\boldsymbol{B}^*$ are set to be less than a predefined value of I to satisfy the homogenization criterion, the criterion can be expressed as follows:

$$-I * \text{Tsai modulus} \le (U_2 * \xi_1^B + U_3 * \xi_2^B) \le I * \text{Tsai modulus} \tag{30}$$

$$-I * \text{Tsai modulus} \le (-U_2 * \xi_1^B + U_3 * \xi_2^B) \le I * \text{Tsai modulus} \tag{31}$$

$$-I * \text{Tsai modulus} \le (-U_3 * \xi_2^B) \le I * \text{Tsai modulus} \tag{32}$$

$$-I * \text{Tsai modulus} \le \left(\frac{1}{2}U_2 * \xi_3^B + U_3 * \xi_4^B\right) \le I * \text{Tsai modulus} \tag{33}$$

$$-I * \text{Tsai modulus} \le \left(\frac{1}{2}U_2 * \xi_3^B - U_3 * \xi_4^B\right) \le I * \text{Tsai modulus} \tag{34}$$

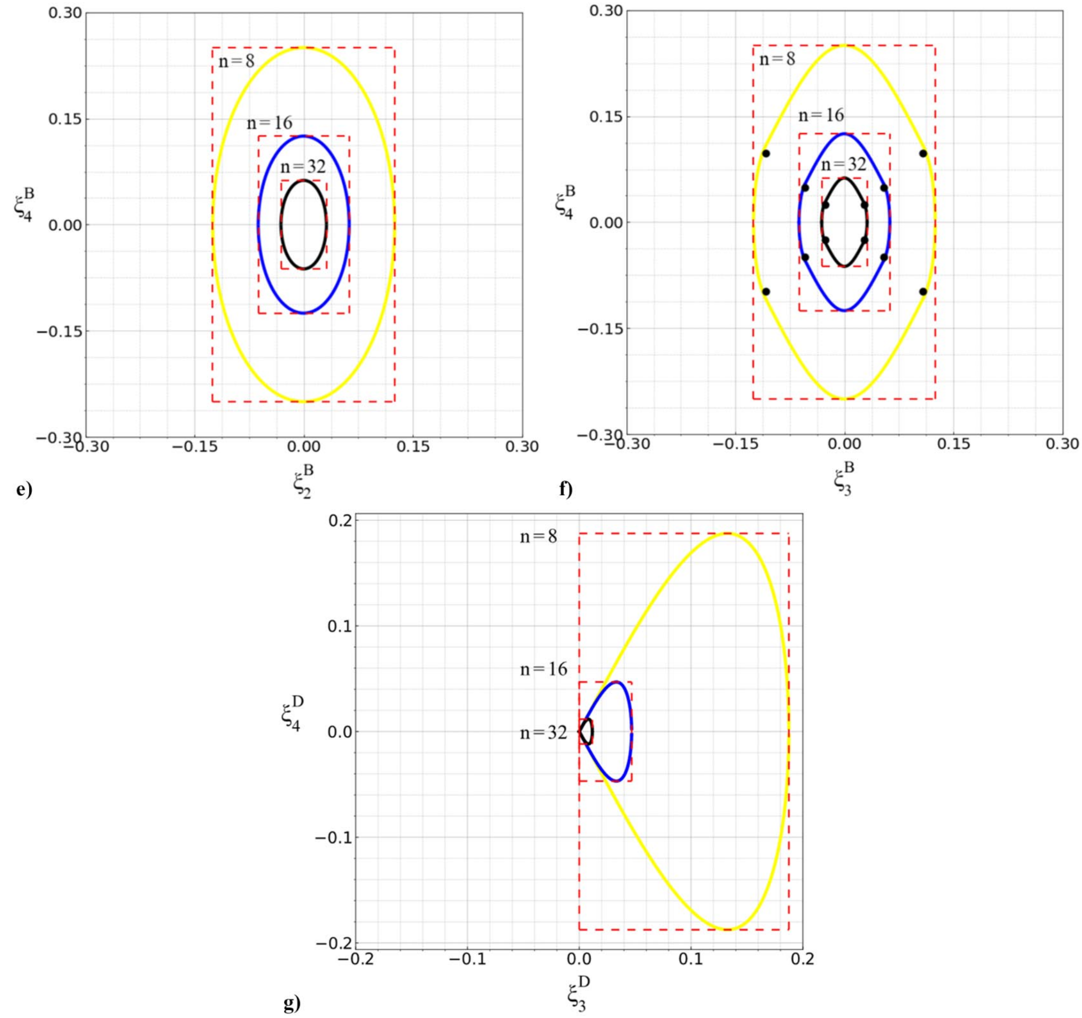

Fig. 5 (Continued).

Table 1 Feasible region boundaries for staggered 1

(x, y)	Feasible region	Range
ξ_1^B, ξ_2^B	$\lvert y\rvert = \frac{1}{n}[(1-2n\lvert x\rvert)^2 - 1]$	$-\frac{1}{n} \le x \le \frac{1}{n}; -\frac{1}{n} \le y \le \frac{1}{n}$
ξ_1^B, ξ_3^B	$n^2y^2 + (2nx \pm 1)^2 = 1$	$-\frac{1}{n} \le x \le \frac{1}{n}; -\frac{1}{n} \le y \le \frac{1}{n}$
ξ_1^B, ξ_4^B	$y = \frac{2}{n}(2nx \pm 1)\sqrt{1-(2nx \pm 1)^2}$ $y = 4x\sqrt{1-(nx)^2}$	$-\frac{1}{n} \le x \le \frac{1}{n}; -\frac{2}{n} \le y \le \frac{2}{n}$
ξ_3^B, ξ_2^B	$y = \pm nx^2$ $y = -2x \pm nx^2$	$-\frac{1}{n} \le x \le \frac{1}{n}; -\frac{1}{n} \le y \le \frac{1}{n}$
ξ_2^B, ξ_4^B	$\left(\frac{y}{2}\right)^2 + x^2 = \frac{1}{n^2}$	$-\frac{1}{n} \le x \le \frac{1}{n}; -\frac{2}{n} \le y \le \frac{2}{n}$
ξ_3^B, ξ_4^B	$y = \pm 2x\sqrt{1-(nx)^2}$ $y = \frac{2}{n}\left(\lvert s_1\sqrt{1-s_1^2} - s_2\sqrt{1-s_2^2}\rvert\right)$ $s_1 = \frac{n}{2}x - \delta, s_2 = \frac{n}{2}x + \delta$ $\delta = \sqrt{(1+\frac{n^2}{4}x^2) - \sqrt{n^2x^2 + \frac{1}{4}}}$	$-\frac{1}{n} \le x \le \frac{1}{n}; -\frac{2}{n} \le y \le \frac{2}{n}$
ξ_3^D, ξ_4^D	$y = 2\lvert x\rvert\sqrt{1-\frac{n^4x^2}{144}}$	$-\frac{12}{n^2} \le x \le \frac{12}{n^2}; -\frac{12}{n^2} \le y \le \frac{12}{n^2}$

From Eqs. (30–32),

$$-\frac{I}{U_2^*} \le \xi_1^B \le \frac{I}{U_2^*} \tag{35a}$$

and

$$-\frac{I}{U_3^*} \le \xi_2^B \le \frac{I}{U_3^*} \tag{35b}$$

where U_2^* and U_3^* are normalized U_2 and U_3 by the Tsai modulus [11].

These are extreme values. The feasible region of (ξ_1^B, ξ_2^B) is a parallelogram with vertices at

$$\left(-\frac{I}{U_2^*}, 0\right), \left(0, -\frac{I}{U_3^*}\right), \left(\frac{I}{U_2^*}, 0\right), \quad \text{and} \quad \left(0, \frac{I}{U_3^*}\right)$$

Combining Eq. (33) and Eq. (34),

$$-\frac{2I}{U_2^*} \le \xi_3^B \le \frac{2I}{U_2^*} \tag{36a}$$

and

$$-\frac{I}{U_3^*} \le \xi_4^B \le \frac{I}{U_3^*} \tag{36b}$$

These are extreme values. The feasible region of (ξ_3^B, ξ_4^B) is a parallelogram with vertices at

$$\left(-\frac{2I}{U_2^*}, 0\right), \left(0, -\frac{I}{U_3^*}\right), \left(\frac{2I}{U_2^*}, 0\right) \quad \text{and} \quad \left(0, \frac{I}{U_3^*}\right)$$

As for the homogenization criterion defined in Eq. 32, $\xi_{3,4}^D$ are inversely proportional to the second order of the number of plies; hence, ξ_3^D and ξ_4^D are always smaller than ξ_3^B and ξ_4^B, respectively. Therefore, for staggered 1, when $[\boldsymbol{B}^*]$ has met the criterion of 2%, $\|[\boldsymbol{A}^*] - [\boldsymbol{D}^*]\|$ is naturally less than 2% of the Tsai modulus. Figure 6 presents the feasible regions in terms of $\xi_{1,2,3,4}^B$ for DD laminates with

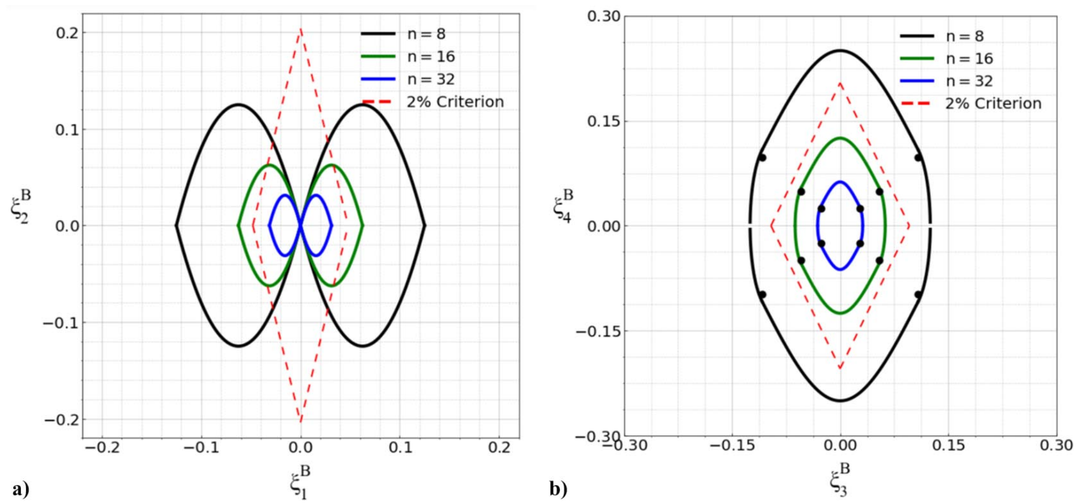

Fig. 6 Feasible regions of $\xi_{1,2,3,4}^B$ with 2% homogenization criterion.

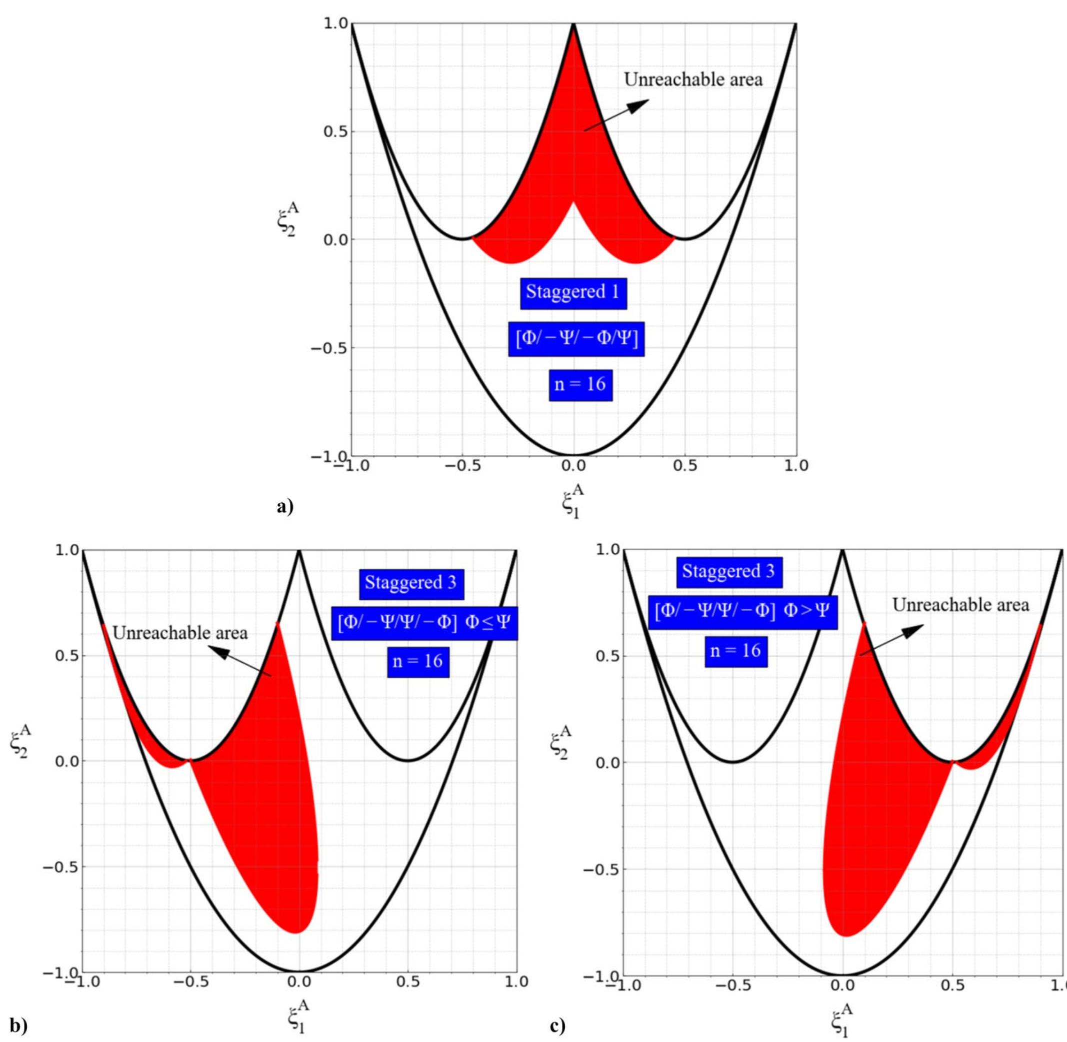

Fig. 7 Unreachable feasible region under 2% homogenization criterion for four-repeat DD laminates on ξ_1^A vs ξ_2^A.

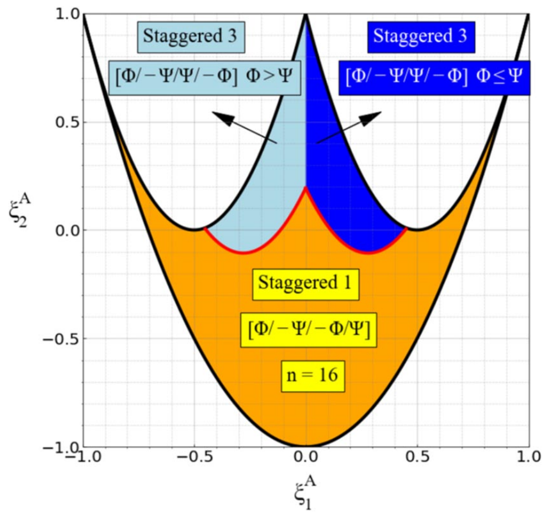

Fig. 8 A tailored feasible region for a combination of staggered 1 and 3.

8, 16, and 32 plies with a homogenization criterion (red dashed line) of 2% of the Tsai modulus replaced by master ply values [11] (i.e., $U_2^* = 0.417$ and $U_3^* = 0.098$), leading to homogenization criterion at $(-0.048, 0)$, $(0, -0.204)$, $(0.048, 0)$, and $(0, 0.204)$ for the feasible region of (ξ_1^B, ξ_2^B) and $(-0.096, 0)$, $(0, -0.204)$, $(0.096, 0)$, and $(0, 0.204)$ for the feasible region of (ξ_3^B, ξ_4^B).

As discussed in Sec. IV.B, the DD laminate with a larger number of plies has smaller design spaces in terms of $\xi_{1,2,3,4}^B$; hence, the homogenization criterion can be relatively easily achieved by the laminates with a larger number of plies/repeats. It can be seen that, for staggered 1 with 16 plies (four repeats), most of the design space is located inside the region defined by the homogenization criterion; whereas for DD laminates with 32 plies (eight repeats), the design space is fully covered by the homogenization criterion.

For the feasible regions out of this homogenization criterion envelope, other types of DD laminates can be employed instead to cover this area; and 16 plies (four repeats) are enough for DD families to reach homogenization. Thus, DD laminates can still retain the maximum design space in bending and extension stiffness while having minimum or no effect on coupling stiffness. By such means, staggered 1 can reach homogenization at 16 plies (four repeats) using staggered 3 as replacements on the unreachable area.

Figure 7 illustrates the unreachable feasible region under 2% homogenization criterion for the four-repeat staggered 1 and 3. For staggered 1, this area in feasible regions ξ_1^B and ξ_2^B is reflected to the feasible regions ξ_1^A and ξ_2^A shown in Fig. 7a. Unlike staggered 1, the unreachable area for staggered 3 is caused by the criterion on ξ_3^B and ξ_4^B rather than ξ_1^B and ξ_2^B. It can be observed that the red area for staggered 1 (see Fig. 7a) can be covered by a combination of staggered 3 when $\Phi \leq \Psi$ (see Fig. 7b) and $\Phi > \Psi$ (see Fig. 7c). Thus, this combination of DD sequences shown in Fig. 8 allows DD laminates to reach all the possible design space covered by the 2% homogenization criterion in just 16 plies (four repeats). As for the conventional QUAD laminates that are characterized as heterogeneous, they would require at least 120 plies to reach homogenization; the large number of plies makes their optimization design hard to perform [1]. Great benefits can therefore be obtained by replacing QUAD laminates with DD laminates.

V. Conclusions

In this study, novel formulations for obtaining the lamination parameters of DD laminates are presented: based on which, the feasible regions of the combinations of any two lamination parameters are obtained analytically using Lagrange multipliers. All the feasible regions with regard to two lamination parameters have been obtained in this paper, and the six typical feasible regions have been presented; whereas the rest are defined by either rotating or scaling these basic shapes. These novel formulations are applicable to all DD laminates, including those with rigid-body rotation, which will be discussed in future work. The proposed method is validated against one of the most popular DD laminates with the stacking sequence of the sublaminate as $[+\phi/-\psi/-\phi/+\psi]$. The obtained results indicate that the lamination parameters ξ_1^A and ξ_2^A are always equal to lamination parameters ξ_1^D and ξ_2^D, respectively, whereas ξ_3^A and ξ_4^A are always zeros. The feasible regions of ξ_{1234}^B have first-order negative correlations with the number of plies. Such a feature is highly beneficial for DD laminates to achieve homogenization. Besides, based on the simple expressions of lamination parameters, feasible regions for any two lamination parameters can be obtained analytically using the method of Lagrange multipliers. Finally, the homogenization criterion of 2% has been drawn in the feasible region of DD laminates, and combination sequences of staggered 1 and 3 have been proved to be able to reach all the design space covered by the 2% homogenization criterion with only 16 plies (four repeats).

Appendix A: A List of 10 Solution Types for Feasible Regions of General DD Laminates

There are 10 possible types, as given in the following list, where superscripts x and y equal A, B, or D and denote the lamination parameters to be plotted on the x and y axes, respectively:

Type (1,1) compares ξ_1^x and ξ_1^y: $f(\theta_1, \theta_2) = p_1 c_1 + p_2 c_2$; $g(\theta_1, \theta_2) = q_1 c_1 + q_2 c_2$.

Type (2,2) compares ξ_2^x and ξ_2^y: $f(\theta_1, \theta_2) = p_1 C_1 + p_2 C_2$; $g(\theta_1, \theta_2) = q_1 C_1 + q_2 C_2$.

Type (3,3) compares ξ_3^x and ξ_3^y: $f(\theta_1, \theta_2) = p_1 s_1 + p_2 s_2$; $g(\theta_1, \theta_2) = q_1 s_1 + q_2 s_2$.

Type (4,4) compares ξ_4^x and ξ_4^y: $f(\theta_1, \theta_2) = p_1 S_1 + p_2 S_2$; $g(\theta_1, \theta_2) = q_1 S_1 + q_2 S_2$.

Type (1,2) compares ξ_1^x and ξ_2^y: $f(\theta_1, \theta_2) = p_1 C_1 + p_2 C_2$; $g(\theta_1, \theta_2) = q_1 c_1 + q_2 c_2$.

Type (1,3) compares ξ_1^x and ξ_3^y: $f(\theta_1, \theta_2) = p_1 s_1 + p_2 s_2$; $g(\theta_1, \theta_2) = q_1 c_1 + q_2 c_2$.

Type (1,4) compares ξ_1^x and ξ_4^y: $f(\theta_1, \theta_2) = p_1 S_1 + p_2 S_2$; $g(\theta_1, \theta_2) = q_1 c_1 + q_2 c_2$.

Type (3,2) compares ξ_3^x and ξ_2^y: $f(\theta_1, \theta_2) = p_1 C_1 + p_2 C_2$; $g(\theta_1, \theta_2) = q_1 s_1 + q_2 s_2$.

Type (2,4) compares ξ_2^x and ξ_4^y: $f(\theta_1, \theta_2) = p_1 S_1 + p_2 S_2$; $g(\theta_1, \theta_2) = q_1 C_1 + q_2 C_2$.

Type (3,4) compares ξ_2^x and ξ_4^y: $f(\theta_1, \theta_2) = p_1 S_1 + p_2 S_2$; $g(\theta_1, \theta_2) = q_1 s_1 + q_2 s_2$, where

$$c_1 = \cos(2\theta_1) \qquad c_2 = \cos(2\theta_2),$$
$$C_1 = \cos(4\theta_1) = 2c_1^2 - 1 = 1\text{–}2s_1^2 \qquad C_2 = \cos(4\theta_2) = 2c_2^2 - 1 = 1\text{–}2s_2^2$$
$$s_1 = \sin(2\theta_1) \qquad s_2 = \sin(2\theta_2)$$
$$S_1 = \sin(4\theta_1) = 2c_1 s_1 \qquad S_2 = \sin(4\theta_2) = 2c_2 s_2$$

and (p_1, p_2) and (q_1, q_2) are the coefficients of the trigonometric functions in the objective function and constraint, respectively.

Appendix B: Feasible Regions of Lamination Parameters

The specific solutions for the DD laminates are $-90 \leq \phi$ and $\psi \leq 90$.

There is no need to compare a parameter with itself. Also, $\xi_1^A = \xi_1^D$, $\xi_2^A = \xi_2^D$ and $\xi_3^A = \xi_4^A = 0$. So, there are 28 comparisons [i.e., $C(8,2) = 28$] between the pairs of the four $\xi_{1,2,3,4}^D$ parameters and the four $\xi_{1,2,3,4}^B$ parameters.

Note that, the solutions in Table B1 are for DD laminates with angles ranging from −90 to 90 deg. Each feasible region for staggered 1, staggered 2, and staggered 3, and paired can be simply achieved by adding angle constraints (0 or 90 deg) onto the boundaries.

Table B1 Feasible regions of different combinations of lamination parameters

x	q_1	q_2	y	p_1	p_2	Type	$-90 \le \phi, \psi \le 90$
ξ_1^D	$\frac{1}{2}$	$\frac{1}{2}$	ξ_1^B	$-\frac{1}{2n}$	$\frac{1}{2n}$	(1,1)	$\lvert y\rvert \le \frac{1}{n}(1-\lvert x\rvert)$
ξ_2^D	$\frac{1}{2}$	$\frac{1}{2}$	ξ_2^B	$-\frac{1}{2n}$	$\frac{1}{2n}$	(2,2)	$\lvert y\rvert \le \frac{1}{n}(1-\lvert x\Big\rvert\Big)$
ξ_3^D	$\frac{6}{n^2}$	$\frac{6}{n^2}$	ξ_3^B	$-\frac{1}{n}$	$\frac{1}{n}$	(3,3)	$\lvert y\rvert \le \left(\frac{2}{n}-\frac{n}{6}\lvert x\rvert\right)$
ξ_4^D	$\frac{6}{n^2}$	$\frac{6}{n^2}$	ξ_4^B	$-\frac{1}{n}$	$\frac{1}{n}$	(4,4)	$\lvert y\rvert \le \left(\frac{2}{n}-\frac{n}{6}\lvert x\rvert\right)$
ξ_1^D	$\frac{1}{2}$	$\frac{1}{2}$	ξ_2^D	$\frac{1}{2}$	$\frac{1}{2}$	(1,2)	$2x^2-1 \le y \le (1\text{–}2\lvert x\rvert)^2$
ξ_1^D	$\frac{1}{2}$	$\frac{1}{2}$	ξ_2^B	$-\frac{1}{2n}$	$\frac{1}{2n}$	(1,2)	$\lvert y\rvert \le \frac{1}{n}[(1\text{–}2\lvert x\rvert)^2-1]$
ξ_1^B	$-\frac{1}{2n}$	$\frac{1}{2n}$	ξ_2^D	$\frac{1}{2}$	$\frac{1}{2}$	(1,2)	$2n^2x^2-1 \le y \le (1\text{–}2n\lvert x\rvert)^2$
ξ_1^B	$-\frac{1}{2n}$	$\frac{1}{2n}$	ξ_2^B	$-\frac{1}{2n}$	$\frac{1}{2n}$	(1,2)	$\lvert y\rvert \le \frac{1}{n}[(1\text{–}2n\lvert x\rvert)^2-1]$
ξ_1^D	$\frac{1}{2}$	$\frac{1}{2}$	ξ_3^D	$\frac{6}{n^2}$	$\frac{6}{n^2}$	(1,3)	$\lvert y\rvert \le \frac{12}{n^2}\sqrt{1-x^2}$
ξ_1^D	$\frac{1}{2}$	$\frac{1}{2}$	ξ_3^B	$-\frac{1}{n}$	$\frac{1}{n}$	(1,3)	$\lvert y\rvert \le \frac{2}{n}\sqrt{1-x^2}$
ξ_1^B	$-\frac{1}{2n}$	$\frac{1}{2n}$	ξ_3^D	$\frac{6}{n^2}$	$\frac{6}{n^2}$	(1,3)	$\lvert y\rvert \le \frac{12}{n^2}\sqrt{1-n^2x^2}$
ξ_1^B	$-\frac{1}{2n}$	$\frac{1}{2n}$	ξ_3^B	$-\frac{1}{n}$	$\frac{1}{n}$	(1,3)	$\lvert y\rvert \le \frac{2}{n}\sqrt{1-n^2x^2}$
ξ_1^D	$\frac{1}{2}$	$\frac{1}{2}$	ξ_4^D	$\frac{6}{n^2}$	$\frac{6}{n^2}$	(1,4)	$\lvert y\rvert \le \max\left[\frac{24\lvert x\rvert}{n^2}\sqrt{1-x^2}, \frac{12}{n^2}\left(\left\lvert c_1\sqrt{1-c_1^2}-c_2\sqrt{1-c_2^2}\right\rvert\right)\right]$ $c_1 = x-\delta, c_2 = x+\delta$ $\delta = \sqrt{(1+x^2)-\sqrt{4x^2+\frac{1}{4}}}$
ξ_1^D	$\frac{1}{2}$	$\frac{1}{2}$	ξ_4^B	$-\frac{1}{n}$	$\frac{1}{n}$	(1,4)	$\lvert y\rvert \le \max\left[\frac{4\lvert x\rvert}{n}\sqrt{1-x^2}, \frac{2}{n}\left(\left\lvert c_1\sqrt{1-c_1^2}-c_2\sqrt{1-c_2^2}\right\rvert\right)\right]$ $c_1 = x-\delta, c_2 = x+\delta$ $\delta = \sqrt{(1+x^2)-\sqrt{4x^2+\frac{1}{4}}}$
ξ_1^B	$-\frac{1}{2n}$	$\frac{1}{2n}$	ξ_4^D	$\frac{6}{n^2}$	$\frac{6}{n^2}$	(1,4)	$\lvert y\rvert \le \max\left[\frac{24\lvert x\rvert}{n}\sqrt{1-n^2x^2}, \frac{12}{n^2}\left(\left\lvert c_1\sqrt{1-c_1^2}-c_2\sqrt{1-c_2^2}\right\rvert\right)\right]$ $c_1 = nx-\delta, c_2 = nx+\delta$ $\delta = \sqrt{(1+(nx)^2)-\sqrt{4n^2x^2+\frac{1}{4}}}$
ξ_1^B	$-\frac{1}{2n}$	$\frac{1}{2n}$	ξ_4^B	$-\frac{1}{n}$	$\frac{1}{n}$	(1,4)	$\lvert y\rvert \le \max\left[4\lvert x\rvert\sqrt{1-n^2x^2}, \frac{2}{n}\left(\left\lvert c_1\sqrt{1-c_1^2}-c_2\sqrt{1-c_2^2}\right\rvert\right)\right]$ $c_1 = nx-\delta, c_2 = nx+\delta$ $\delta = \sqrt{(1+(nx)^2)-\sqrt{4n^2x^2+\frac{1}{4}}}$
ξ_3^D	$\frac{6}{n^2}$	$\frac{6}{n^2}$	ξ_2^D	$\frac{1}{2}$	$\frac{1}{2}$	(3,2)	$-\left(1-\frac{n^2\lvert x\rvert}{6}\right)^2 \le y \le 1-\frac{n^4x^2}{72}$
ξ_3^D	$\frac{6}{n^2}$	$\frac{6}{n^2}$	ξ_2^B	$-\frac{1}{2n}$	$\frac{1}{2n}$	(3,2)	$\lvert y\rvert \le \frac{1}{n}\left[1-\left(1-\frac{n^2\lvert x\rvert}{6}\right)^2\right]$
ξ_3^B	$-\frac{1}{n}$	$\frac{1}{n}$	ξ_2^D	$\frac{1}{2}$	$\frac{1}{2}$	(3,2)	$-(1-n\lvert x\rvert)^2 \le y \le 1-\frac{n^2}{2}x^2$
ξ_3^B	$-\frac{1}{n}$	$\frac{1}{n}$	ξ_2^B	$-\frac{1}{2n}$	$\frac{1}{2n}$	(3.2)	$\lvert y\rvert \le \frac{1}{n}(1-n\lvert x\rvert)^2$
ξ_2^D	$\frac{1}{2}$	$\frac{1}{2}$	ξ_4^D	$\frac{6}{n^2}$	$\frac{6}{n^2}$	(2,4)	$\lvert y\rvert \le \frac{12}{n^2}\sqrt{1-x^2}$
ξ_2^D	$\frac{1}{2}$	$\frac{1}{2}$	ξ_4^B	$-\frac{1}{n}$	$\frac{1}{n}$	(2,4)	$\lvert y\rvert \le \frac{2}{n}\sqrt{1-x^2}$
ξ_2^B	$-\frac{1}{2n}$	$\frac{1}{2n}$	ξ_4^D	$\frac{6}{n^2}$	$\frac{6}{n^2}$	(2,4)	$\lvert y\rvert \le \frac{12}{n^2}\sqrt{1-n^2x^2}$

Table B1 (*Continued.*)

x	q_1	q_2	y	p_1	p_2	Type	$-90 \le \phi, \psi \le 90$
ξ_2^B	$-\frac{1}{2n}$	$\frac{1}{2n}$	ξ_4^B	$-\frac{1}{n}$	$\frac{1}{n}$	(2,4)	$\lvert y\rvert \le \frac{2}{n}\sqrt{1-n^2x^2}$
ξ_3^D	$\frac{6}{n^2}$	$\frac{6}{n^2}$	ξ_4^D	$\frac{6}{n^2}$	$\frac{6}{n^2}$	(3,4)	$\lvert y\rvert \le \max\left[2\lvert x\rvert\sqrt{1-\frac{n^4x^2}{144}}, \frac{12}{n^2}\left(\left\lvert s_1\sqrt{1-s_1^2}-s_2\sqrt{1-s_2^2}\right\rvert\right)\right]$ $s_1=\frac{n^2}{12}x-\delta, s_2=\frac{n^2}{12}x+\delta$ $\delta=\sqrt{\left(1+\frac{n^4x^2}{144}\right)-\sqrt{\frac{n^4x^2}{36}+\frac{1}{4}}}$
ξ_3^D	$\frac{6}{n^2}$	$\frac{6}{n^2}$	ξ_4^B	$-\frac{1}{n}$	$\frac{1}{n}$	(3,4)	$\lvert y\rvert \le \max\left[\frac{n\lvert x\rvert}{3}\sqrt{1-\frac{n^4x^2}{144}}, \frac{2}{n}\left(\left\lvert s_1\sqrt{1-s_1^2}-s_2\sqrt{1-s_2^2}\right\rvert\right)\right]$ $s_1=\frac{n^2}{12}x-\delta, s_2=\frac{n^2}{12}x+\delta$ $\delta=\sqrt{\left(1+\frac{n^4x^2}{144}\right)-\sqrt{\frac{n^4x^2}{36}+\frac{1}{4}}}$
ξ_3^B	$-\frac{1}{n}$	$\frac{1}{n}$	ξ_4^D	$\frac{6}{n^2}$	$\frac{6}{n^2}$	(3,4)	$\lvert y\rvert \le \max\left[\frac{12\lvert x\rvert}{n}\sqrt{1-\frac{n^2}{4}x^2}, \frac{12}{n^2}\left(\left\lvert s_1\sqrt{1-s_1^2}-s_2\sqrt{1-s_2^2}\right\rvert\right)\right]$ $s_1=\frac{n}{2}x-\delta, s_2=\frac{n}{2}x+\delta$ $\delta=\sqrt{\left(1+\frac{n^2}{4}x^2\right)-\sqrt{n^2x^2+\frac{1}{4}}}$
ξ_3^B	$-\frac{1}{n}$	$\frac{1}{n}$	ξ_4^B	$-\frac{1}{n}$	$\frac{1}{n}$	(3,4)	$\lvert y\rvert \le \max\left[2\lvert x\rvert\sqrt{1-\frac{n^2}{4}x^2}, \frac{2}{n}\left(\left\lvert s_1\sqrt{1-s_1^2}-s_2\sqrt{1-s_2^2}\right\rvert\right)\right]\Big]$ $s_1=\frac{n}{2}x-\delta, s_2=\frac{n}{2}x+\delta$ $\delta=\sqrt{\left(1+\frac{n^2}{4}x^2\right)-\sqrt{n^2x^2+\frac{1}{4}}}$

References

[1] Tsai, S. W., "Double–Double: New Family of Composite Laminates," *AIAA Journal*, Vol. 59, No. 11, 2021, pp. 4293–4305. https://doi.org/10.2514/1.J060659

[2] Herakovich, C. T., "Mechanics of Composites: A Historical Review," *Mechanics Research Communications*, Vol. 41, April 2012, pp. 1–20. https://doi.org/10.1016/j.mechrescom.2012.01.006

[3] Abdalla, M. M., Kassapoglou, C., and Gürdal, Z., "Formulation of Composite Laminate Robustness Constraint in Lamination Parameters Space," *AIAA/ASME/ASCE/AHS/ASC Structures, Structural Dynamics and Materials Conference*, AIAA Paper 2009-2478, May 2009, pp. 1–15. https://doi.org/10.2514/6.2009-2478

[4] Irisarri, F. X., Bassir, D. H., Carrere, N., and Maire, J. F., "Multiobjective Stacking Sequence Optimization for Laminated Composite Structures," *Composites Science and Technology*, Vol. 69, Nos. 7–8, 2009, pp. 983–990. https://doi.org/10.1016/j.compscitech.2009.01.011

[5] Liu, D., Toropov, V. V., Barton, D. C., and Querin, O. M., "Weight and Mechanical Performance Optimization of Blended Composite Wing Panels Using Lamination Parameters," *Structural and Multidisciplinary Optimization*, Vol. 52, No. 3, 2015, pp. 549–562. https://doi.org/10.1007/s00158-015-1244-x

[6] Macquart, T., Bordogna, M. T., Lancelot, P., and de Breuker, R., "Derivation and Application of Blending Constraints in Lamination Parameter Space for Composite Optimisation," *Composite Structures*, Vol. 135, Jan. 2016, pp. 224–235. https://doi.org/10.1016/j.compstruct.2015.09.016

[7] Macquart, T., Werter, N., and de Breuker, R., "Aeroelastic Design of Blended Composite Structures Using Lamination Parameters," *Journal of Aircraft*, Vol. 54, No. 2, 2017, pp. 561–571. https://doi.org/10.2514/1.C033859

[8] Bordogna, M. T., Lancelot, P., Bettebghor, D., and de Breuker, R., "Static and Dynamic Aeroelastic Tailoring with Composite Blending and Manoeuvre Load Alleviation," *Structural and Multidisciplinary Optimization*, Vol. 61, No. 5, 2020, pp. 2193–2216. https://doi.org/10.1007/s00158-019-02446-w

[9] Meddaikar, Y. M., Irisarri, F.-X., and Abdalla, M. M., "Laminate Optimization of Blended Composite Structures Using a Modified Shepard's Method and Stacking Sequence Tables," *Structural and Multidisciplinary Optimization*, Vol. 55, No. 2, 2017, pp. 535–546. https://doi.org/10.1007/s00158-016-1508-0

[10] Ijsselmuiden, S. T., Abdalla, M. M., Seresta, O., and Gürdal, Z., "Multi-Step Blended Stacking Sequence Design of Panel Assemblies with Buckling Constraints," *Composites Part B: Engineering*, Vol. 40, No. 4, 2009, pp. 329–336. https://doi.org/10.1016/j.compositesb.2008.12.002

[11] Tsai, S. W., Melo, J. D. D., Sihn, S., Arteiro, A., and Rainsberger, R., *Composite Laminates: Theory and Practice of Analysis, Design and Automated Layup*, Stanford Univ. Dept. of Aeronautics and Astronautics, Stanford, CA, 2017, p. 45.

[12] Vermes, B., Tsai, S. W., Riccio, A., di Caprio, F., and Roy, S., "Application of the Tsai's Modulus and Double-Double Concepts to the Definition of a New Affordable Design Approach for Composite Laminates," *Composite Structures*, Vol. 259, Nov. 2020, 2021, Paper 113246. https://doi.org/10.1016/j.compstruct.2020.113246

[13] Shrivastava, S., Sharma, N., Tsai, S. W., and Mohite, P. M., "D and DD-Drop Layup Optimization of Aircraft Wing Panels Under Multi-Load Case Design Environment," *Composite Structures*, Vol. 248, Jan. 2020, Paper 112518. https://doi.org/10.1016/j.compstruct.2020.112518

[14] Bloomfield, M. W., Diaconu, C. G., and Weaver, P. M., "On Feasible Regions of Lamination Parameters for Lay-Up Optimization of Laminated Composites," *Proceedings of the Royal Society of London, Series A: Mathematical, Physical and Engineering Sciences*, Vol. 465, No. 2104, 2009, pp. 1123–1143. https://doi.org/10.1098/rspa.2008.0380

[15] Diaconu, C. G., Sato, M., and Sekine, H., "Feasible Region in General Design Space of Lamination Parameters for Laminated Composites," *AIAA Journal*, Vol. 40, No. 3, 2002, pp. 559–565.

[16] Diaconu, C. G., and Sekine, H., "Layup Optimization for Buckling of Laminated Composite Shells with Restricted Layer Angles," *AIAA Journal*, Vol. 42, No. 3, 2004, pp. 2153–2163.

[17] Ijsselmuiden, S. T., Abdalla, M. M., and Gürdal, Z., "Implementation of Strength-Based Failure Criteria in the Lamination Parameter Design Space," *AIAA Journal*, Vol. 46, No. 7, 2008, pp. 1826–1834. https://doi.org/10.2514/1.35565

[18] York, C. B., "Laminate Stiffness Tailoring for Improved Buckling Performance," *Thin-Walled Structures*, Vol. 161, Nov. 2021, Paper 107482. https://doi.org/10.1016/j.tws.2021.107482

[19] Tsai, S. W., and Pagano, N. J., "Invariant Properties of Composite Materials," Tech. Rept., U.S. Air Force Materials Lab., Wright–Patterson AFB, OH, 1968.

[20] Grenestedt, J. L., and Gudmundson, P., "Layup Optimization of Composite Material Structures," *Optimal Design with Advanced Materials*, Elsevier, New York, 1993, pp. 311–336. https://doi.org/10.1016/b978-0-444-89869-2.50027-5

[21] Svanberg, K., *On Local and Global Minima in Structural Optimization*, Royal Inst. of Technology, Stockholm, Sweden, 1981, pp. 327–341.

[22] Albazzan, M. A., Harik, R., Tatting, B. F., and Gürdal, Z., "Efficient Design Optimization of Nonconventional Laminated Composites Using Lamination Parameters: A State of the Art," *Composite Structures*, Vol. 209, Feb. 2019, pp. 362–374. https://doi.org/10.1016/j.compstruct.2018.10.095

[23] Dutra, T. A., and de Almeida, S. F. M., "Composite Plate Stiffness Multicriteria Optimization Using Lamination Parameters," *Composite Structures*, Vol. 133, Dec. 2015, pp. 166–177. https://doi.org/10.1016/j.compstruct.2015.07.029

[24] Fukunaga, H., Sekine, H., Sato, M., and Iino, A., "Buckling Design of Symmetrically Laminated Plates Using Lamination Parameters," *Computers and Structures*, Vol. 57, No. 4, 1995, pp. 643–649. https://doi.org/10.1016/0045-7949(95)00050-Q

[25] Jin, P., Zhong, X., Yang, J., and Sun, Z., "Blending Design of Composite Panels with Lamination Parameters," *Aeronautical Journal*, Vol. 120, No. 1233, 2016, pp. 1710–1725. https://doi.org/10.1017/aer.2016.88

[26] Kameyama, M., and Fukunaga, H., "Optimum Design of Composite Plate Wings for Aeroelastic Characteristics Using Lamination Parameters," *Computers and Structures*, Vol. 85, Nos. 3–4, 2007, pp. 213–224. https://doi.org/10.1016/j.compstruc.2006.08.051

[27] Liu, B., Haftka, R. T., and Trompette, P., "Maximization of Buckling Loads of Composite Panels Using Flexural Lamination Parameters," *Structural and Multidisciplinary Optimization*, Vol. 26, No. 1, 2004, pp. 28–36. https://doi.org/10.1007/s00158-003-0314-7

[28] Liu, D., and Toropov, V. V., "A Lamination Parameter-Based Strategy for Solving an Integer-Continuous Problem Arising in Composite Optimization," *Computers and Structures*, Vol. 128, Nov. 2013, pp. 170–174. https://doi.org/10.1016/j.compstruc.2013.06.003

[29] Todoroki, A., and Sasai, M., "Stacking Sequence Optimizations Using GA with Zoomed Response Surface on Lamination Parameters," *Advanced Composite Materials*, Vol. 11, No. 3, 2002, pp. 299–318. https://doi.org/10.1163/156855102762506335

[30] Xu, Y., Zhu, J., Wu, Z., Cao, Y., Zhao, Y., and Zhang, W., "A Review on the Design of Laminated Composite Structures: Constant and Variable Stiffness Design and Topology Optimization," *Advanced Composites and Hybrid Materials*, Vol. 1, No. 3, 2018, pp. 460–477. https://doi.org/10.1007/s42114-018-0032-7

[31] Hao, P., Liu, D., Wang, Y., Liu, X., Wang, B., Li, G., and Feng, S., "Design of Manufacturable Fiber Path for Variable-Stiffness Panels Based on Lamination Parameters," *Composite Structures*, Vol. 219, July 2019, pp. 158–169. https://doi.org/10.1016/j.compstruct.2019.03.075

[32] Shahabad, P. K., Anamagh, M. R., and Bediz, B., "Design of Laminated Conical Shells Using Spectral Chebyshev Method and Lamination Parameters," *Composite Structures*, Vol. 281, Feb. 2022, Paper 114969. https://doi.org/10.1016/j.compstruct.2021.114969

[33] Zeng, J., Huang, Z., Fan, K., and Wu, W., "An Adaptive Hierarchical Optimization Approach for the Minimum Compliance Design of Variable Stiffness Laminates Using Lamination Parameters," *Thin-Walled Structures*, Vol. 157, Dec. 2020, Paper 107068. https://doi.org/10.1016/j.tws.2020.107068

[34] Silva, G. H. C., and Meddaikar, Y., "Lamination Parameters for Sandwich and Hybrid Material Composites," *AIAA Journal*, Vol. 58, No. 10, 2020, pp. 4604–4611. https://doi.org/10.2514/1.J059093

[35] Liu, X., Featherston, C. A., and Kennedy, D., "Two-Level Layup Optimization of Composite Laminate Using Lamination Parameters," *Composite Structures*, Vol. 211, March 2019, pp. 337–350. https://doi.org/10.1016/j.compstruct.2018.12.054

[36] Miki, M., "Material Design of Composite Laminates with Required In-Plane Elastic Properties," *Progress in Science and Engineering of Composites*, Vol. 2, Japan Soc. for Composite Materials, Tokyo, 1982, pp. 1725–1731.

[37] Miki, M., *Design of Laminated Fibrous Composite Plates with Required Flexural Stiffness*, ASTM International, West Conshohocken, PA, 1985, pp. 387–400.

[38] Fukunaga, H., and Sekine, H., "Stiffness Design Method of Symmetric Laminates Using Lamination Parameters," *AIAA Journal*, Vol. 30, No. 11, 1992, pp. 2791–2793. https://doi.org/10.2514/3.11304

[39] Fukunaga, H., and Sekine, H., "A Laminate Design for Elastic Properties of Symmetric Laminates with Extension-Shear or Bending-Twisting Coupling," *Journal of Composite Materials*, Vol. 28, No. 8, 1994, pp. 708–731. https://doi.org/10.1177/002199839402800802

[40] Diaconu, C. G., Sato, M., and Sekine, H., "Feasible Region in General Design Space of Lamination Parameters for Laminated Composites," *AIAA Journal*, Vol. 40, No. 3, 2002, pp. 559–565.

[41] Setoodeh, S., Abdalla, M. M., and Gürdal, Z., "Approximate Feasible Regions for Lamination Parameters," *Collection of Technical Papers—11th AIAA/ISSMO Multidisciplinary Analysis and Optimization Conference*, Vol. 2, 2006, pp. 814–822; also AIAA Paper 2006-6973, Sept. 2006. https://doi.org/10.2514/6.2006-6973

[42] Bloomfield, M. W., Herencia, J. E., and Weaver, P. M., "Analysis and Benchmarking of Meta-Heuristic Techniques for Lay-Up Optimization," *Computers and Structures*, Vol. 88, Nos. 5–6, 2010, pp. 272–282.

[43] Tsai, S. W., and Melo, J. D. D., "An Invariant-Based Theory of Composites," *Composites Science and Technology*, Vol. 100, Aug. 2014, pp. 237–243. https://doi.org/10.1016/j.compscitech.2014.06.017

R. Ohayon
Associate Editor